Applied Mathematics & Information Sciences
An International Journal

http://dx.doi.org/10.18576/amis/190415

Parameter Estimation and Global Sensitivity Analysis for Transmission Dynamics of Avian Influenza in Humans and Domestic Birds

S. P. Soka[1,*], *M. Mayengo*[2], *and M. Kgosimore*[3]

[1]Moshi Secondary School, P.O.Box 3021 Moshi-Tanzania
[2]School of Computational and Communication Science and Engineering, The Nelson Mandela African, Institution of Science and Technology (NM-AIST) P.O.Box 447 Arusha-Tanzania
[3]Department of Biometry and Mathematics, Botswana University of Agriculture and Natural Resources, it Private Bag 0027 Gaborone Botswana

Received: 7 Jan. 2025, Revised: 21 May 2025, Accepted: 9 Apr. 2025
Published online: 1 Jul. 2025

Abstract: The aim of the study was to derive insights on the transmission dynamics and make realistic predictions of avian influenza as influenced by human and domestic birds, accounting for the effects of environmental factors and contribute to mitigation strategies against avian influenza. Steady-state solutions were examined to determine the equilibrium conditions of the system. The basic reproduction number was computed using the next-generation matrix method to characterize the outcomes of the disease transmission dynamics. The least squares and Latin Hypercube Sampling-Partial Rank Correlation Coefficient methods were used to carry out sensitivity analysis of the model to efficiently estimate and identify influential parameters on the model outputs. Numerical simulations were performed to demonstrate the dynamical trends of avian influenza under various scenarios. The research findings revealed that the spread of avian influenza is directly influenced by human interaction with a contaminated environment, the level of infectiousness of birds, and the shedding of the virus by infected birds, all of which are directly proportional to the overall spread of avian influenza disease. The stability conditions established in terms of the basic reproduction number played a critical role in determining the dynamics and severity of influenza outbreaks

Keywords: Avian influenza, mathematical model, parameter estimation, stability analysis, transmission dynamics

1 Introduction

Avian influenza (AI) is a viral infection that mainly affects birds but can infect humans and other animals [1]. It is caused by influenza viruses of type A, which are categorized into two sub-types, namely hemagglutinin (H) and neuraminidase (N). Avian influenza viruses are classified into two groups based on pathogenicity: low-pathogenic avian influenza (LPAI), which causes mild illness, and highly pathogenic avian influenza (HPAI), which results in severe disease and high mortality rates in domestic birds and humans [2]. Among avian influenza strains, the H5N1 and H7N9 strains are particularly dangerous due to their high mortality rates in birds and their ability to cause severe illness and death in infected humans [2]. Migratory wild birds, such as waterfowl and shorebirds, are natural reservoirs of AI viruses and are usually released into the environment. These viruses can spread to domestic birds either through direct contact with infected wild birds or via environments contaminated by migrating wild birds [3]. Humans become infected through close contact with infected birds or their secretions, as well as contaminated environments [3,5]. Typical symptoms of avian influenza in domestic birds include coughing, sneezing, swelling, decreased egg production, and sudden death [4]. Infected humans with HPAI exhibit symptoms such as fever, cough, sore throat, and muscle aches. In severe cases, breathing difficulties and pneumonia can develop in infected individuals. The severity of symptoms depends on the virus strain and the individual's health [6,8].

The disease severely affects various countries, including Tanzania, leading to economic and social

* Corresponding author e-mail: sokas@nm-aist.ac.tz

challenges, as many families rely on domestic bird farming for their livelihoods [7]. The outbreak of avian influenza in various parts of the country poses a significant challenge to affected farmers, leading to high mortality and decreased production. The recurrence of avian influenza, therefore, impacts both the financial well-being of farming communities and the general availability of essential nutrition [7]. In essence, avian influenza creates a a significant economic burden on society, such as opportunity losses, health-related expenses, and unemployment. Meanwhile, the costs associated with the implementation of control measures, such as vaccination, treatment, and educational campaigns, are also high. Furthermore, culling of entire flocks during outbreaks of avian influenza can be an emotionally distressing experience (mental health) for families who have devoted substantial time and energy to the care of these birds.

Various researchers from different countries have developed numerous mathematical models to estimate parameters and analyze the transmission dynamics of avian influenza ([27], [36], [37]). Hobbelen et al. [29] estimated the farm–specific time windows for the introduction of highly pathogenic avian influenza into poultry flocks using deterministic and stochastic modeling approaches. Sara et al. [31] carried out parameter estimation and sensitivity analysis of influenza A transmission dynamics. Bonney et al. [30] estimated epidemiological parameters using diagnostic testing data from low pathogenicity avian influenza-infected turkeys, where a stochastic model approach was used. The results indicated that transmission parameters play the most significant role on the spread of the disease. These studies further, revealed that multiple factors impact the dynamics of avian influenza in various countries, along with efficiency of strategies for controlling and managing the disease. These studies have revealed multiple factors that can impact the dynamics of avian influenza in various countries, along with strategies for controlling and managing the disease. Although mathematical models have been extensively used to study avian influenza, the role of domestic birds in understanding disease dynamics has received less attention in the literature. The aim of the study was to derive insights on the transmission dynamics and make realistic predictions of avian influenza as influenced by human and domestic birds, accounting for the effects of environmental factors and contribute to mitigation strategies against AI.

This paper is structured as follows; Section 2 introduces the materials and methods used, Section 3 examines the results and discussions.

2 Materials and Methods

In this section, a system of nonlinear differential equations was introduced and solved using the ODE45 method. In addition, least-squares, LHS and PRCC techniques were employed for parameter estimation and global sensitivity analysis.

2.1 Model Formulation

Fig. 1 shows the routes of transmission of avian influenza between humans and domestic bird populations. The human population is divided into three groups, namely: susceptible population (S_h), infectious population (I_h) and recovered population (R_h). The susceptible human population is replenished at a recruitment rate (Λ_1), which includes new individuals entering through births and migration. Furthermore, individuals who recover from the infection but gradually lose immunity at a rate (ψ) return to the susceptible class. However, this population is reduced by the natural deaths rate (μ_1) and by the force of infection (λ_1), which represents the rate at which susceptible individuals become infected and move to another states. The force of infection is defined by

$$\lambda_1 = \gamma_1 I_d + \gamma_2 B. \tag{1}$$

Where γ_1 represents the rate at which susceptible humans are infected through direct contact with infected domestic birds, while γ_2 refers to the rate of transmission from environments contaminated by infected humans (I_h) and infected domestic birds (I_d). The infected population (I_h) increases due to the force of infection (λ_1) but decreases due to the natural death rate (μ_1), the disease-induced death rate (ε), and the recovery rate (α). The recovered population (R_h) increases as a result of the recovery rate (α). However, it decreases due to the natural death rate (μ_1) and the rate of immunity loss (ψ).

The domestic bird population is divided into two groups: susceptible to infection (S_d) class and infected (I_d) class. There is no recovered group in the model because highly pathogenic avian influenza (HPAI) outbreaks are so severe that they result in the total loss of the domestic bird population [18]. The susceptible group increases at a recruitment rate (Λ_2) but is reduced by natural deaths (μ_2) and force of infection (λ_2) as defined by

$$\lambda_2 = \beta_1 B + \beta_2 I_d. \tag{2}$$

Where β_1 represents the rate at which susceptible domestic birds become infected through exposure to the environment contaminated by infected humans (I_h) and infected domestic birds (I_d), while β_2 refers to the transmission rate through direct contact with infected birds. The infected class (I_d) declines rapidly as a result of the disease-induced rate (τ). The environment (B) becomes contaminated with avian influenza viruses mainly due to migratory wild birds, such as waterfowl and shorebirds, which act as natural carriers, primarily spreading low-pathogenic avian influenza (LPAI) strains [3]. When these birds are infected with highly pathogenic avian influenza (HPAI), they release the virus through bodily fluids, increasing environmental contamination with the more strains [32]. Infected humans and domestic birds also release the virus into the environment through their secretions, at rates (δ_1) and (δ_2), respectively. Moreover, avian influenza viruses naturally decrease in the environment at a decay rate (σ).

The model is formulated by considering the following assumptions: direct interaction between susceptible domestic birds and infected wild birds is not considered, as the focus is on the transmission dynamics of avian influenza through environments contaminated by migratory wild birds, which serve as natural reservoirs of the virus and release it into the environment [3]; direct human-to-human transmission of avian influenza is disregarded due to its rare occurrence [24]; the exposed classes are disregarded in the analysis due to the short incubation period [25].

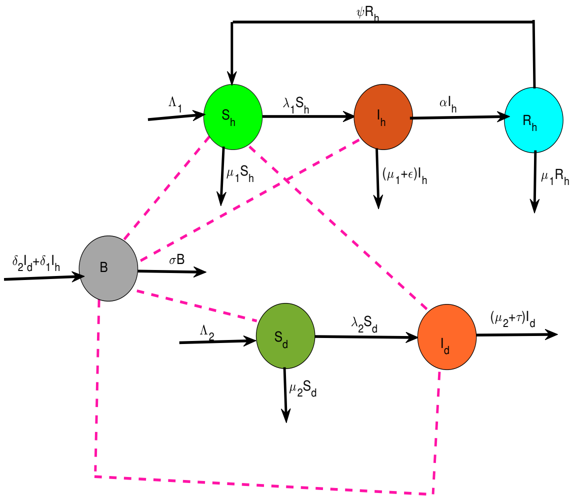

Fig. 1: Compartmental flow diagram for the transmission dynamics of avian influenza

The transmission dynamics of avian influenza are presented by a non-linear system of ordinary differential equations.

$$\begin{cases} \dot{S}_h = \Lambda_1 + \psi R_h - (\mu_1 + \lambda_1) S_h, \\ \dot{I}_h = \lambda_1 S_h - (\mu_1 + \varepsilon + \alpha) I_h, \\ \dot{R}_h = \alpha I_h - (\psi + \mu_1) R_h, \\ \dot{S}_d = \Lambda_2 - (\mu_2 + \lambda_2) S_d, \\ \dot{I}_d = \lambda_2 S_d - (\mu_2 + \tau) I_d, \\ \dot{B} = \delta_2 I_d + \delta_1 I_h - \sigma B. \end{cases} \tag{3}$$

Using initial conditions; $S_h(0) > 0$; $I_h(0) \geq 0$; $R_h(0) \geq 0$; $S_d(0) > 0$; $I_d(0) \geq 0$; and $B \geq 0$.

2.2 *Model analysis*

2.2.1 Invariant region

Consider the total human population; $N_h(t) = S_h(t) + I_h(t) + R_h(t)$

$$\frac{dN_h}{dt} = \Lambda_1 - \mu_1 N_h - \varepsilon I_h \tag{4}$$

Solving the equation (4), subject to the initial conditions, we get

$$N_h(t) \leq \frac{\Lambda_1}{\mu_1} + \left(N_h(0) - \frac{\Lambda_1}{\mu_1} \right) e^{-\mu_1 t} \tag{5}$$

As $t \to \infty$ in equation (5), $N_h(t) \to \frac{\Lambda_1}{\mu_1}$, thus

$$0 < N_h(t) \leq \frac{\Lambda_1}{\mu_1}. \tag{6}$$

The same procedures used for the domestic bird population, $0 < N_d(t) \leq \frac{\Lambda_2}{\mu_2}$. If $N_d(t) \leq \frac{\Lambda_2}{\mu_2}$ and $N_h(t) \leq \frac{\Lambda_1}{\mu_1}$ it indicates that $I_h(t) \leq \frac{\Lambda_1}{\mu_1}$ and $I_d(t) \leq \frac{\Lambda_2}{\mu_2}$. Maintaining generality, it shows that $B \leq \frac{\delta_1 \Lambda_1}{\sigma \mu_1} + \frac{\delta_2 \Lambda_2}{\sigma \mu_2}$. The closed set Γ given as $\Gamma = \{(S_h, I_h, R_h, S_d, I_d, B) \in \mathbb{R}^6_+ : N_h \leq \frac{\Lambda_1}{\mu_1}, N_d \leq \frac{\Lambda_2}{\mu_2}, B \leq \frac{\delta_1 \Lambda_1}{\sigma \mu_1} + \frac{\delta_2 \Lambda_2}{\sigma \mu_2}\}$. Γ is a feasible region of the model (3) that is considered as epidemiological and mathematically well-posed.

2.2.2 Positivity of the model solution

We demonstrate that the solution of the model remains non-negative for all t ≥ 0.

Theorem 2.1. Given that; $S_h(0) > 0$, $I_h(0) > 0$, $R_h(0) > 0$, $S_d(0) > 0$, $I_d(0) > 0$, $B(0) > 0$ the solution set $\{S_h(t)$, $I_h(t)$, $R_h(t)$, $S_d(t)$, $I_d(t)$, $B(t)\}$ for the model equation (3) remains non-negative for all t ≥ 0.

Proof. $\frac{dS_h}{dt} = \Lambda_1 + \psi_1 R_h - (\mu_1 + \lambda_1) S_h$

$$\frac{dS_h}{dt} \geq -(\mu_1 + \lambda_1) S_h \tag{7}$$

Through integration and application of initial conditions, equation (7) becomes;

$$S_h \geq S_h(0) e^{-\int_0^t (\mu_1 + \lambda_1) ds} > 0,$$

Applying the same procedures to the remaining equations in model (3), it can be proven that the model solutions are positive for all $t \geq 0$

2.2.3 Disease free equilibrium (E^0) and basic reproduction number (R_0)

When avian influenza is absent in populations, a free disease steady state denoted by E^0 is given by $E^0 = \left(\frac{\Lambda_1}{\mu_1}, 0, 0, \frac{\Lambda_2}{\mu_2}, 0, 0\right)$.
In epidemiological setting, the spread of avian influenza in the population is determined by the basic reproduction number R_0. The basic reproduction number refers to the number of secondary infectious cases that arise when a single primary infected individual is introduced into a population of susceptible individuals [9,26]. The value of R_0 is calculated using the next-generation matrix method, $\frac{dx_i}{dt} = \mathscr{F}(x_i) - \mathscr{V}(x_i)$ where, $\mathscr{F}(x_i)$ represents the arrival of newly infected individuals into the compartment i and $\mathscr{V}(x_i)$ denotes the individuals who exit or leave the compartment i by all other means, $i = \{1,2,3\}$. $F = \frac{\partial \mathscr{F}_i(E^0)}{\partial x_j}$ and $V = \frac{\partial \mathscr{V}_i(E^0)}{\partial x_j}$

$$F= \begin{pmatrix} 0 & \frac{\gamma_1\Lambda_1}{\mu_1} & \frac{\gamma_2\Lambda_1}{\mu_1} \\ 0 & \frac{\beta_2\Lambda_2}{\mu_2} & \frac{\beta_1\Lambda_2}{\mu_2} \\ 0 & 0 & 0 \end{pmatrix} \text{ and } V = \begin{pmatrix} \mu_1+\varepsilon+\alpha & 0 & 0 \\ 0 & \mu_2+\tau & 0 \\ -\delta_1 & -\delta_2 & \sigma \end{pmatrix}$$

The largest non-negative eigenvalue from FV^{-1} matrix denoted as $\rho(FV^{-1}) = R_0$.
From model (3), we obtain

$$FV^{-1} = \begin{pmatrix} r_{11} & r_{12} & r_{13} \\ r_{21} & r_{22} & r_{23} \\ 0 & 0 & 0 \end{pmatrix} \quad (8)$$

where,

$$r_{11} = r_{13}\left(\frac{\delta_1}{\mu_1+\varepsilon+\alpha}\right),$$
$$r_{12} = r_{13}\left(\frac{\gamma_1\sigma}{\gamma_2(\mu_2+\tau)} + \frac{\delta_2}{\mu_1+\varepsilon+\alpha}\right),$$
$$r_{13} = \frac{\gamma_2\Lambda_1}{\mu_1\sigma},$$
$$r_{21} = r_{23}\left(\frac{\delta_1}{\mu_1+\varepsilon+\alpha}\right),$$
$$r_{22} = \frac{r_{23}}{\mu_2+\tau}\left(\frac{\beta_2\sigma}{\beta_1} + \delta_2\right),$$
$$r_{23} = \frac{\beta_1\Lambda_2}{\mu_2\sigma}.$$

From equation (8), the polynomial characteristic is obtained as shown in equation (9).

$$\lambda^3 - (r_{22}+r_{11})\lambda^2 - (-r_{11}r_{22} + r_{12}r_{21})\lambda = 0 \quad (9)$$

solving equation (9), the spectral radius is;

$$R_0 = \frac{r_{11} + r_{22} + \sqrt{(r_{11}-r_{22})^2 + 4r_{12}r_{21}}}{2} \quad (10)$$

The quantities r_{11}, r_{22}, r_{12}, and r_{21} in equation (10) represent the contributions to the basic reproduction number (R_0) from both within and between compartments. Specifically, quantities r_{11} and r_{22} denote the sub-basic reproduction number within a single group, signifying the direct or indirect infection of susceptible individuals by infected members of the same group. On the other hand, quantities r_{12} and r_{21} represent the interactions between the two groups, showing how individuals from one group can infect individuals in the other group, either directly or indirectly.

2.2.4 Local stability of the disease free equilibrium

Theorem 2.2. The disease free equilibrium for the avian influenza model system (3) is locally asymptotically stable if $R_0 < 1$ and unstable if $R_0 > 1$.

Proof. The proof follows the approach used in Ruoja et al. [35], and van den Driessche and Watmough [14]. From Theorem 2 of van den Driessche and Watmough [14] , we have that V and F in section 2.2.3 are non-singular M-matrix and non-negative, respectively. However matrix $V-F$ has Z pattern which implies that $(V-F)V^{-1}$ $=I-FV^{-1}$ is a Z pattern sign matrix. Additionally by Lemma 5 of van den Driessche and Watmough [14], we have that both $V-F$ and $I-FV^{-1}$ are non-singular M-matrix implying that $\rho(FV^{-1}) < 1$. This implies that, the disease free equilibrium for the avian influenza model system (3) is locally asymptotically stable.

2.2.5 Global stability of the disease free equilibrium

Theorem 2.3. The disease free equilibrium (E^0) is globally asymptotically stable when $R_0 < 1$ and unstable otherwise.

Proof. We examine the global stability of disease free equilibrium of model (3) by utilizing the method given by Castillo-Chavez et al [16]. The model system (3) is written in the form of;

$$\begin{cases} \frac{dY_m}{dt} = C_1(Y_m - Y_{DFE}) + C_2Y_n \\ \frac{dY_n}{dt} = C_3Y_n \end{cases}$$

where,
Y_m indicates non-transmitting avian influenza compartments; Y_n indicates transmitting avian influenza compartments; and Y_{DFE} denotes disease-free equilibrium. If matrix C_1 has real negative eigenvalues and C_3 is a Metzler matrix (i.e., the off-diagonal entries are positive), then the avian influenza free equilibrium is globally asymptotically stable.

From model system (3):
$Y_m = (S_h, R_h, S_d)^T$ and $Y_n = (I_h, I_d, B)^T$

$$(Y_m - Y_{(DFE)}) = \begin{bmatrix} S_h - \frac{\Lambda_1}{\mu_1} \\ R_h \\ S_d - \frac{\Lambda_2}{\mu_2} \end{bmatrix}$$

$$C_2 = \begin{bmatrix} 0 & \dfrac{\gamma_1\Lambda_1}{\mu_1} & \dfrac{\gamma_2\Lambda_1}{\mu_1} \\ \alpha & 0 & 0 \\ 0 & \dfrac{\beta_2\Lambda_2}{\mu_2} & \dfrac{\beta_1\Lambda_2}{\mu_2} \end{bmatrix}$$

We investigate whether matrix C_1 for non-transmitting classes has real negative eigenvalues and C_3 is a Metzler matrix.

$$C_1 = \begin{pmatrix} -\mu_1 & \psi & 0 \\ 0 & -(\psi+\mu_1) & 0 \\ 0 & 0 & -\mu_2 \end{pmatrix}$$

$$C_3 = \begin{pmatrix} -(\mu_1+\varepsilon+\alpha) & \dfrac{\gamma_1\Lambda_1}{\mu_1} & \dfrac{\gamma_2\Lambda_1}{\mu_1} \\ 0 & -\left((\mu_2+\tau) - \dfrac{\beta_2\Lambda_2}{\mu_2}\right) & \dfrac{\beta_1\Lambda_2}{\mu_2} \\ \delta_1 & \delta_2 & -\sigma \end{pmatrix}$$

The eigenvalues of matrix C_1 are $\lambda_1 = -\mu_1$, $\lambda_2 = -(\psi+\mu_1)$, $\lambda_3 = -\mu_2$

It can be observed that the eigenvalues of matrix C_1 are negative, and C_3 is a Metzler matrix. This indicates that the disease-free equilibrium of the model system (3) is globally asymptotically stable.

2.2.6 Disease endemic equilibrium (E^*)

Endemic equilibrium is a situation in epidemiology where the disease exists within the population. By setting LHS of the model system (3) to zero, and writing equations I_h^*, I_d^* and B^* in terms of λ_1^* and λ_2^*, observed that

$$\begin{cases} \lambda_1^* = \gamma_1 I_d^* + \gamma_2 B^* \\ \lambda_2^* = \beta_1 B^* + \beta_2 I_d^* \end{cases} \tag{11}$$

Eliminating B^* from equation (11) and make simplifications, it shows that

$$\lambda_2^* = \left(\frac{\beta_1(\mu_2+\tau)}{(\beta_1\gamma_1 - \beta_2\gamma_2)S_d^* + (\mu_2+\tau)\gamma_2} \right) \lambda_1^* \tag{12}$$

Thus;

$$\begin{cases} I_h^* = \left(\dfrac{S_h^*}{\mu_1+\varepsilon+\alpha}\right)\lambda_1^* \\ I_d^* = \left(\dfrac{S_d^*}{\mu_2+\tau}\right)\lambda_2^* \\ B^* = \dfrac{\delta_2}{\sigma}\left(\dfrac{S_d^*}{\mu_2+\tau}\right)\lambda_2^* + \dfrac{\delta_1}{\sigma}\left(\dfrac{S_h^*}{\mu_1+\varepsilon+\alpha}\right)\lambda_1^* \end{cases}$$

2.2.7 Stability of Endemic Equilibrium (E^*)

The local stability of the disease-free equilibrium (DFE) is maintained if $R_0 < 1$ and becomes unstable when $R_0 > 1$. Consequently, by revising this condition, the endemic equilibrium (EE) is locally stable if $R_0 > 1$ and unstable when $R_0 < 1$ [10]. The global stability of endemic equilibrium in epidemiology refers to the study of the behavior of an infectious disease within the population.

Theorem 2.4. If $R_0 > 1$, then the endemic equilibrium point (E^*) of the avian influenza model system (3) is globally asymptotically stable in Γ.

Proof. Lyapunov function for the avian influenza model system 3 is constructed using Nyerere et al. [10], Trazias et al. [33] and Bada et al. [13] approach. We employed the Lyapunov function of the form;

$$L = \Sigma_{i=1}^n G_i \left(x_i - x_i^* - x_i^* \ln\left(\frac{x_i}{x_i^*}\right)\right)$$

where;

G_i is positive constant, x_i is the variable in the compartment i, for $i = \{1,2,3,4,5,6\}$ and x_i^* refers to the compartment variable at the equilibrium point.

The Lyapunov function using model system (3) is defined as

$$\begin{aligned} L = {} & G_1\left(S_h - S_h^* - S_h^*\ln\left(\frac{S_h}{S_h^*}\right)\right) \\ & + G_2\left(I_h - I_h^* - I_h^*\ln\left(\frac{I_h}{I_h^*}\right)\right) \\ & + G_3\left(R_h - R_h^* - R_h^*\ln\left(\frac{R_h}{R_h^*}\right)\right) \\ & + G_4\left(S_d - S_d^* - S_d^*\ln\left(\frac{S_d}{S_d^*}\right)\right) \\ & + G_5\left(I_d - I_d^* - I_d^*\ln\left(\frac{I_d}{I_d^*}\right)\right) \\ & + G_6\left(B - B^* - B^*\ln\left(\frac{B}{B^*}\right)\right) \end{aligned}$$

assuming that; $G_1 = G_2 = G_3 = G_4 = G_5 = G_6 = 1$. The time derivative of Lyapunov L becomes

$$\begin{aligned} \frac{dL}{dt} = {} & \left(1 - \frac{S_h^*}{S_h}\right)[\Lambda_1 + \psi R_h - (\mu_1 + \gamma_1 I_d + \gamma_2 B)S_h] \\ & + \left(1 - \frac{I_h^*}{I_h}\right)[(\gamma_1 I_d + \gamma_2 B)S_h - (\mu_1+\varepsilon+\alpha)I_h] \\ & + \left(1 - \frac{R_h^*}{R_h}\right)[\alpha I_h - (\psi+\mu_1)R_h] \\ & + \left(1 - \frac{S_d^*}{S_d}\right)[\Lambda_2 - (\mu_2 + \beta_1 B + \beta_2 I_d)S_d] \\ & + \left(1 - \frac{I_d^*}{I_d}\right)[(\beta_1 B + \beta_2 I_d)S_d - (\mu_2+\tau)I_d] \\ & + \left(1 - \frac{B^*}{B}\right)[\delta_2 I_d + \delta_1 I_h - \sigma B] \end{aligned} \tag{13}$$

By considering the model system (3) at E^*, we have

$$\begin{cases} \Lambda_1 = \left(\mu_1 + \gamma_1 I_d^* + \gamma_2 B^*\right) S_h^* - \psi R_h^*, \\ \mu_1 + \varepsilon + \alpha = \dfrac{(\gamma_1 I_d^* + \gamma_2 B^*) S_h^*)}{I_h^*} \\ \mu_1 + \psi = \dfrac{\alpha I_h^*}{R_h^*}, \\ \Lambda_2 = (\mu_2 + \beta_2 I_d^* + \beta_1 B^*) S_d^*, \\ \mu_2 + \tau = \dfrac{(\beta_2 I_d^* + \beta_1 B^*) S_d^*}{I_D^*}, \\ \sigma = \dfrac{\delta_2 I_d^* + \delta_1 I_h^*}{B^*}. \end{cases} \tag{14}$$

Substitute Equation (14) to (13) and simplify, we obtain;

$$\begin{aligned} \frac{dL}{dt} &= \gamma_1 I_d^* S_h^* \left(2 - \frac{S_h^*}{S_h} + \frac{I_d}{I_d^*} - \frac{I_H}{I_h^*} - \frac{I_d}{I_d^*}\frac{S_h}{S_h^*}\frac{I_h^*}{I_h}\right) \\ &+ \gamma_2 B^* S_h^* \left(2 - \frac{S_H^*}{S_h} + \frac{I_d}{I_d^*} - \frac{I_h}{I_h^*} - \frac{I_d}{I_d^*}\frac{S_h}{S_h^*}\frac{I_h^*}{I_h}\right) \\ &+ \beta_1 B^* S_d^* \left(2 - \frac{S_d^*}{S_d} + \frac{B}{B^*} - \frac{I_d}{I_d^*} - \frac{B}{B^*}\frac{S_d}{S_d^*}\frac{I_d^*}{I_d}\right) \\ &+ \beta_2 I_d^* S_d^* \left(2 - \frac{S_d^*}{S_d} - \frac{S_d}{S_d^*}\right) \\ &+ \mu_1 S_h^* \left(2 - \frac{S_h^*}{S_h} - \frac{S_h}{S_h^*}\right) \\ &+ \mu_2 S_d^* \left(2 - \frac{S_d^*}{S_d} - \frac{S_d}{S_d^*}\right) \\ &+ \delta_1 I_H^* \left(1 - \frac{B}{B^*} + \frac{I_h}{I_h^*} - \frac{B^*}{B}\frac{I_h}{I_h^*}\right) \\ &+ \delta_2 I_d^* \left(1 - \frac{B}{B^*} + \frac{I_d}{I_d^*} - \frac{B^*}{B}\frac{I_d}{I_d^*}\right) \\ &+ \alpha I_h^* \left(1 - \frac{R_h}{R_h^*} + \frac{I_h}{I_h^*} - \frac{R_h^*}{R_h}\frac{I_h}{I_h^*}\right) \\ &+ \psi R_h \left(1 - \frac{S_h^*}{S_h} - \frac{R_h^*}{R_h} + \frac{R_h^*}{R_h}\frac{S_h^*}{S_h}\right) \end{aligned}$$

The relation as utilized by [34] is used,

$1 - x + \ln x \leq 0 \Rightarrow 1 - x \leq -\ln x, \quad \text{for} x \in \mathbb{R}, x > 0$

$\left(1 - \frac{B}{B^*} + \frac{I_h}{I_h^*} - \frac{B^*}{B}\frac{I_h}{I_h^*}\right) \leq 0,$

$\left(1 - \frac{B}{B^*} + \frac{I_h}{I_h^*} - \frac{B^*}{B}\frac{I_h}{I_h^*}\right) =$

$\left(1 - \frac{B}{B^*}\right) + \left(1 - \frac{B^*}{B}\frac{I_h}{I_h^*}\right) + \left(\frac{I_h}{I_h^*} - 1\right) \leq 0$

$= -\ln a \; - \; \ln\left(\frac{b}{a}\right) \; + \; \ln b \quad = -\left(\ln a + \ln\frac{b}{a} - \ln b\right)$

$= -\ln\left(\frac{ab}{ab}\right) = 0$

Thus, $\frac{dL}{dt} \leq 0$, using LaSalle's extension of Lyapunov's method, the limit set of each solution lies within the largest invariant set, where $S_h = S_h^*$, $I_h = I_h^*$, $R_h = R_h^*$, $S_d = S_d^*$, $B = B^*$ which is the singleton E^* [17].

Hence the endemic equilibrium point of the model system (3) is globally asymptotically stable on Γ when $R_0 > 1$.

2.3 Parameter estimation and model fitting

In this section, we employ the least-squares technique to estimate the parameters. The method is well-suited for general parameter estimation. The objective function is to minimize the sum of square residuals expressed as: $(\min \Sigma_{i=1}^{n}[x_i - f(y_{i,\theta})]^2)$; where θ are the parameter values to be estimated from existing literatures; n represent the total number of data points; $f(y_{i,\theta})$ represents the solutions of a nonlinear model function and x_i refers to the artificial generated data obtained by adding Gaussian noise to the model result $(f(y_{i,\theta}))$. We utilize the capabilities offered by MATLAB's built-in function "fminsearch," which employs the Nelder-Mead simplex algorithm to derive local minimizers for the residual sum of squares [28]. The estimated values of the parameters were employed, and the corresponding outcomes are shown in Figs. 2-4. Figs. 2 and 3 demonstrate that as the estimated data more closely aligns with the observed data, the model's accuracy and validity increase. This indicates that it can be used to make reliable predictions about the future trend of the disease.

Fig. 4 indicates that the residuals for all outcomes follow a normal distribution, confirming the stability and reliability of the model fit and parameter values for future use.

2.4 Global sensitivity analysis

In this part, the Latin Hypercube Sampling (LHS) technique and Partial Rank Correlated Coefficient (PRCC) are employed to carry out a global sensitivity analysis of parameters in relation to infected state variables. The LHS technique is employed to generate combinations of 1,000 uniformly distributed samples for the model parameter values [11]. Furthermore, we calculated the Partial Rank Correlation Coefficients between the model parameters and the infected state variables to evaluate if the uncertainties of the parameters make a substantial impact. The PRCC value provides a measure of the impact that a parameter has on the state variable. A PRCC value closer to 1 or -1 suggests a higher degree of influence for a parameter, whereas values within the range of 0.2 to -0.2 show a weaker level of influence [34]. The sign and direction of the PRCC reveal the nature of the influence that a parameter has on the state variable. Positive values show a positive influence; that means whenever the parameter values increase, the outcome increases, and vice versa. On the other hand, negative values indicate a negative influence; this indicates that as parameter values increase, the output decreases. Fig. 5 shows that the environment to human

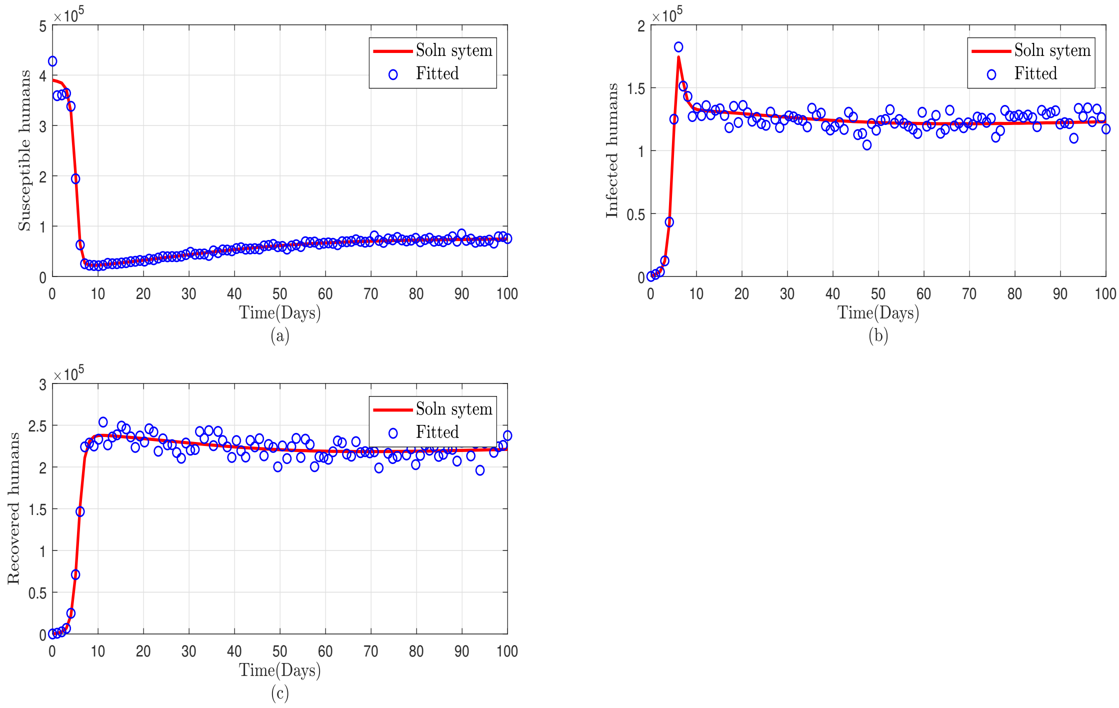

Fig. 2: Model fitting of susceptible, infected and recovered humans population.

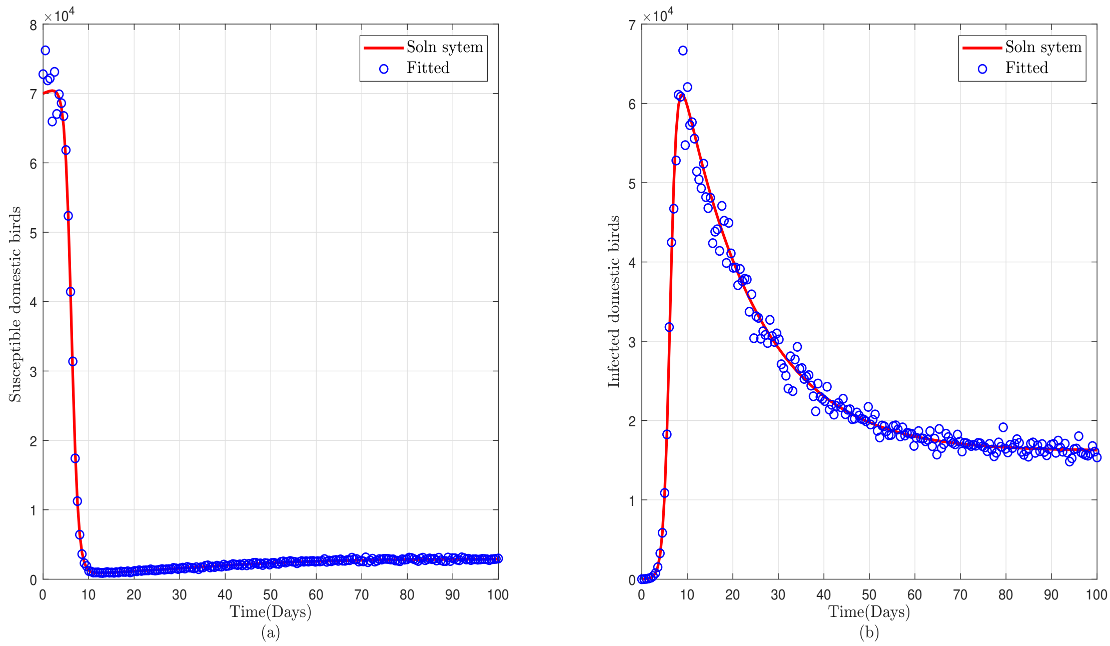

Fig. 3: Model fitting of susceptible and infected domestic birds population.

Table 1: Model baseline and estimated values day^{-1}

Symbol	Baseline	Source	Estimation	(Mean (μ), std (σ))
Λ_1	300	[20]	295.964713	(297.982357, 2.853379)
γ_1	0.00008	[12]	0.000086	(0.000083, 4×10^{-6})
α	0.9	[21]	0.907719	(0.903860, 5.458×10^{-3})
β_1	0.00004	assumed	0.000036	(0.000038, 3×10^{-6})
μ_1	0.0000391	[19]	0.000042	(0.000041, 2×10^{-6})
ε	0.000001	[20]	0.000004	(0.000002, 1×10^{-6})
β_2	0.00002	[22]	0.000027	(0.000042, 5×10^{-6})
ψ	0.5	assumed	0.500806	(0.500403, 5.7×10^{-4})
σ	0.875	[23]	0.854378	(0.864689, 0.014582)
δ_2	0.008	assumed	0.007448	0.007724, 3.9×10^{-4}
Λ_2	1000	[19]	1063.641926	(1031.820963, 45.001637)
δ_1	0.0006	assumed	0.000549	(0,000574, 3.6 $\times10^{-5}$)
μ_2	0.01	[22]	0.010252	(0,010126, 1.78×10^{-4})
τ	0.05	[22]	0.052461	(0.051230, 1.74×10^{-3})
γ_2	0.0008	assumed	0.000860	(0.000830, 4.2×10^{-5})

transmission rate (γ_2), bird to bird transmission rate (β_2), infected human to environment transmission rate (δ_1), environment to domestic bird transmission rate (β_1), and infected bird to human transmission rate (γ_1) have positive PRCC values, which means they are accountable for increasing avian influenza in humans whenever they increase and decreasing avian influenza in humans whenever they decrease Conversely, the natural death rate (μ_1), the human-induced death rate (ε), birds disease induced death rate (τ) and avian influenza virus decay rate (σ) both have negative PRCC values, implying that these parameter values are inversely related to the PRCC values. This means that decreasing the values of these parameters would lead to a increase of the disease in the population. The outcomes from Fig. 6 illustrate that the bird-to-bird transmission rate (β_2) spreads the avian influenza disease throughout the outbreak, while γ_2, δ_1, β_1, and γ_1 contribute to the disease spreading within the first 60 days. To prevent the spread of the avian influenza outbreak, authorities should implement a vaccination program and other control measures such as culling infected domestic birds, promoting proper hygiene practices, and conducting educational campaigns on the disease's impact. From Fig. 7, we observed that the bird-to-bird transmission rate (β_2), recruitment rate (Λ_2), environment to domestic bird transmission rate (β_1), humans to environment transmission rate (δ_1), and domestic to environment transmission rate (δ_2) have positive PRCC values, indicating that an increase in these parameter values leads to a greater spread of avian influenza, and vice versa, while induced death rate (τ), natural death rate (μ_2), avian influenza virus decay rate (σ), and human recovery rate (α) all have negative PRCC values, which suggests that these parameter values are inversely related to the PRCC values. This implies that an increase in these parameter values results in a decrease in the spread of avian influenza. The result from Fig. 8 indicates that β_2 widely spreads the disease throughout the avian influenza outbreak while γ_2, δ_1, and β_1 transmit the disease within the first 68 days. We observe that to reduce the number of domestic bird infection cases during the outbreak, the parameter β_2 should be lowered throughout the entire duration, and parameters such as γ_2, δ_1, and β_1 should be decreased within the first 68 days. Fig. 9 shows that the human-to-environment transmission rate (δ_1), domestic-to-domestic rate (β_2), domestic-to-environment rate (δ_2), and environment-to-domestic rate (β_1) all have positive PRCC. This indicates that the parameter values are directly proportional to the PRCC values. Meanwhile, the virus decay rate (σ), induced death rate (τ), and recovery rate (α) all have negative PRCC values. This shows that these parameter values are inversely related to the PRCC values. The result from Fig. 10 indicates that δ_1, δ_2, and β_2 are crucial factors driving the spread of avian influenza throughout the entire disease outbreak. Furthermore, the environment-to-human rate (γ_2), the infected bird-to-human rate (γ_1), and the environment-to-domestic rate (β_1) emerge as significant contributors to the spread of the avian influenza within the first 58 days of the outbreak. On the other hand, as the virus decay rate (σ) and recovery rate (α) increase, the avian influenza disease decreases.

3 Results and Discussion

In this section, we numerically solved the model system 3 using the ODE45 method implemented in the MATLAB software. The model parameters and their values are shown in Table 1, accompanied by the initial values of the model. Fig. 11 (a) shows that the number of susceptible

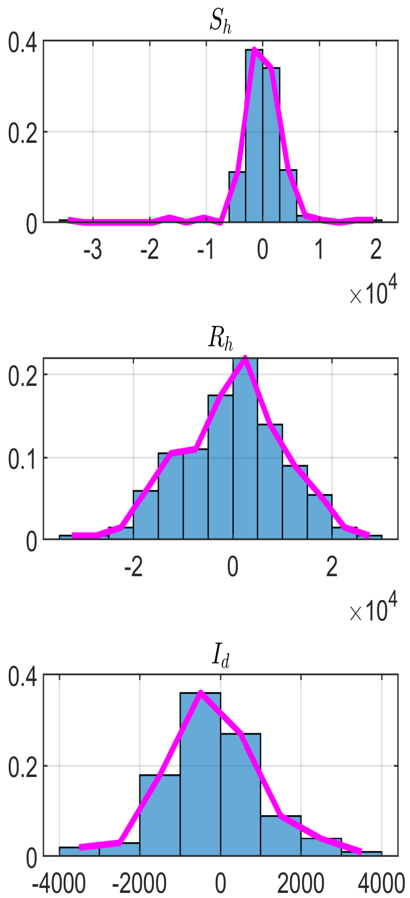

Fig. 4: **The results of the model's residuals.**

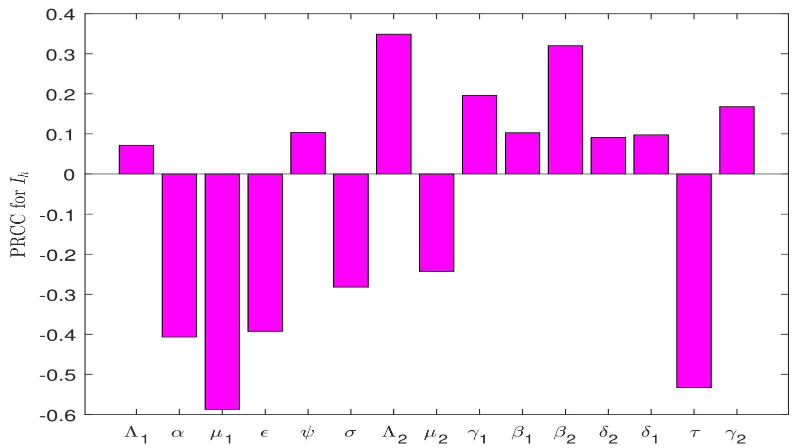

Fig. 5: **Partial rank correlation coefficient for infected humans against model parameters.**

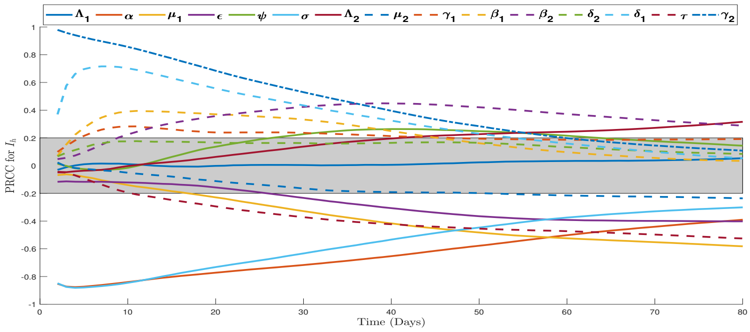

Fig. 6: Partial rank correlation coefficient for infected humans versus time

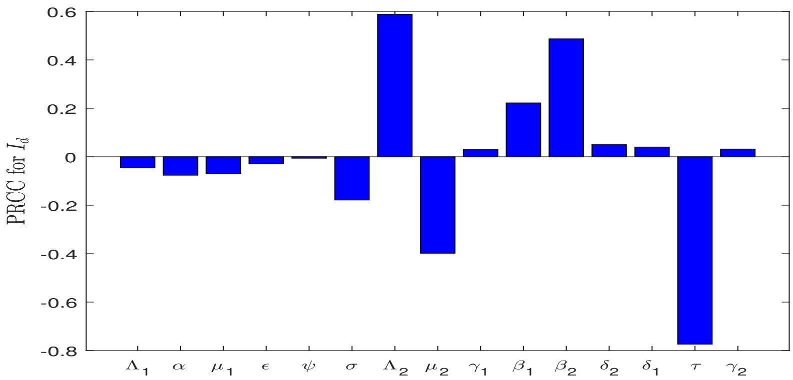

Fig. 7: Partial rank correlation coefficient for infected domestic birds against model parameters.

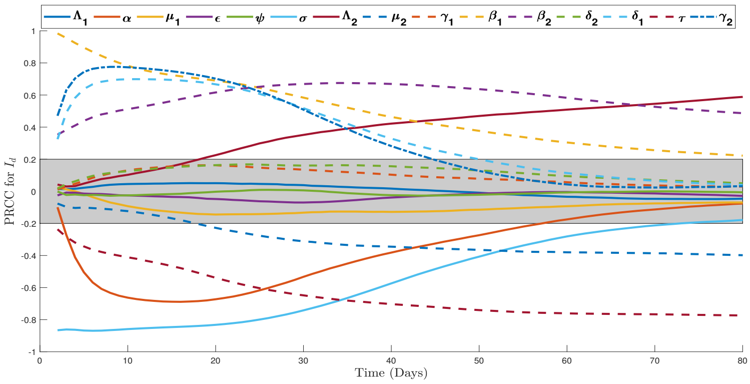

Fig. 8: Partial rank correlation coefficient for infected domestic birds versus time.

humans decreases with time due to the infectiousness of avian influenza. After 12 days, it increases gradually due to immunity loss from the recovering population, until the 70th day, when the whole population stabilizes. Additionally, 11 (b) demonstrates that domestic birds decline abruptly due to the rapid spread of the avian influenza virus. After 50 days, the whole population stabilizes. In Fig. 11 (c), the concentration of avian influenza viruses in the environment rises due to the secretion of viruses from infected domestic birds and humans, reaching a maximum level. Subsequently, the viral concentration decreases to stabilize at a steady state level.

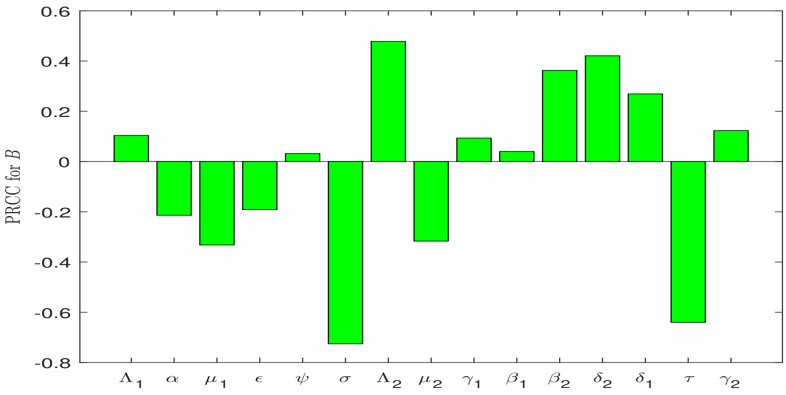

Fig. 9: Partial rank correlation coefficient for contaminated environment against model parameters.

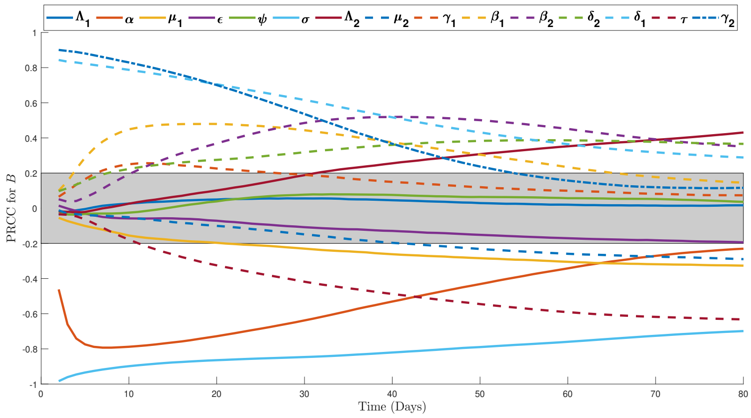

Fig. 10: Partial rank correlation coefficient for contaminated environment versus time

3.1 Conclusion and recommendations

In this paper, we developed and analyzed a mathematical model to examine the dynamics of avian influenza in both human and domestic bird populations. The model system of non-linear differential equations was formulated. The basic reproduction number was computed through the next-generation matrix method. The equilibrium points of model (3) were computed and revealed that, the avian influenza-free equilibrium is globally asymptotically stable when $R_0 < 1$, while the avian influenza endemic equilibrium is globally asymptotically stable when $R_0 > 1$. Moreover, the LHS and PRCC techniques were employed to detect which parameters have a high influence on the spread of avian influenza. The findings showed that an increase in bird-to-bird transmission rate (β_2), shedding rates of infected humans (δ_1) and infected domestic birds (δ_2), environment-to-human rate (γ_2), and environment-to-domestic bird rate (β_1) cause a high influence on the spread of avian influenza. Meanwhile, the human-induced death rate (ε), the disease-induced rate (τ), and the decay rate of viruses (σ) have high negative values, meaning that when they increase, the disease tends to decrease. Based on the observations of avian influenza transmission, we recommend a comprehensive set of measures be implemented. Vaccination programs should be put in place for both human and domestic bird populations. This is crucial in reducing the risk of co-infection with avian influenza viruses. Furthermore, to ensure the continued effectiveness of these vaccines, it is advised to regularly update them in response to the prevailing strains of the virus. This should take into account the mutation characteristics of the influenza strain, as the virus is known to mutate rapidly. Apart from that, the government should take steps to ensure that proper hygiene practices are followed across the relevant sectors. This includes promoting regular handwashing, thorough cleaning, and disinfection of equipment and facilities, as well as restricting access to outsiders who may inadvertently introduce the virus. Maintaining a high standard of

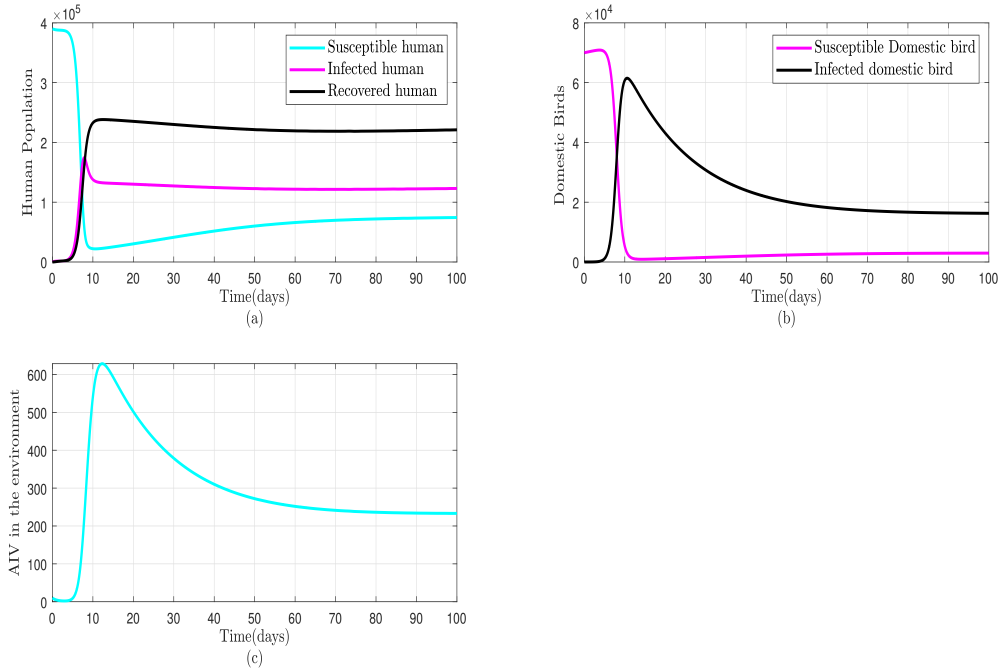

Fig. 11: The transmission dynamics of the avian influenza virus for all compartments.

sanitation and limiting potential points of entry for the disease will be crucial in mitigating its spread. Also, timely culling or isolation of infected domestic birds is necessary to prevent further transmission. Prompt action in identifying and containing infected populations will help prevent the virus from spreading further and reduce the risk of spillover into human communities. The implementation of these measures in a coordinated and comprehensive manner will be essential in addressing the avian influenza outbreak and safeguarding the health and well-being of both human and domestic bird populations.

Acknowledgment

. The authors express their heartfelt gratitude to the Holy Spirit Sisters for their advice and encouragement in this study. We also extend our special appreciation to the Nelson Mandela African Institution of Science and Technology (NM-AIST) for providing a conducive studying environment and the Botswana University of Agriculture and Natural Resources (BUAN) for providing excellent academic support and guidance.

CRediT authorship contribution statement

- Serapia Peter Soka conceptualization, model analysis, writing the first manuscript, editing and submitting the final draft of the manuscript.
- Dr. Maranya M. Mayengo has contributed by providing insightful suggestions on the methodology, reviewing, and editing the manuscript.
- Prof. Moatlhodi Kgosimore has contributed by providing insightful suggestions on the methodology, reviewing, and editing the manuscript.

Funding

There is no funding received for this research.

Declaration of Competing Interest

The authors declare that they have no conflict of interests.

References

[1] A. Samy, & M. M. Naguib, Avian respiratory coinfection and impact on avian influenza pathogenicity in domestic poultry: field and experimental findings. Veterinary sciences, **5**, 23 (2018).

[2] A. Prakash, A. Maan, S. Roy, R. Jha, R. Kumar, & P. Saha, Current Update on Avian Influenza: A Review. International Journal of Pharmacy & Life Sciences, **12**, (2021).

[3] M. Gashaw, A review on avian influenza and its economic and public health impact. International Journal of Veterinary Science & Technology, **4**, 15-27 (2020).

[4] N. Arafat, S. Abd El Rahman, D. Naguib, R. A. El-Shafei, W. Abdo, & A. H. Eladl, Co-infection of Salmonella enteritidis with H9N2 avian influenza virus in chickens. Avian Pathology, **49**, 496-506 (2020).
[5] V. Hénaux, J. Parmley, C. Soos, & M. D. Samuel, Estimating transmission of avian influenza in wild birds from incomplete epizootic data: implications for surveillance and disease spread. Journal of Applied Ecology, **50**, 223-231 (2013).
[6] R. Valensia, I. L. Hilmi, & S. Salman, Analysis of the Effectiveness of Avian Influenza Treatment in Humans: Literature Review. Jurnal eduhealth, **13**, 1137-1142 (2022).
[7] E. S. Sergeant, L. R. Dries, K. M. Moore, & S. E. Salmon, Estimating population sensitivity and confidence of freedom from highly pathogenic avian influenza in the Victorian poultry industry using passive surveillance. Preventive Veterinary Medicine, **202**, 105622 (2022).
[8] C. Ke, C. K. P. Mok, W. Zhu, H. Zhou, J. He, W. Guan, & J. S. M. Peiris, Human infection with highly pathogenic avian influenza A (H7N9) virus, China. Emerging infectious diseases, **23**, 1332 (2017).
[9] F. Branda, M. Pierini, & S. Mazzoli, Monkeypox: Early estimation of basic reproduction number R0 in Europe. Journal of Medical Virology, **95**, e28270, (2023).
[10] N. Nyerere, L. Luboobi, S. Mpeshe, & G. Shirima, Mathematical model for the infectiology of brucellosis with some control strategies. NM-AIST, Tanzania, (2019).
[11] H. Trazias, J. Irunde, M. Kgosimore, & M. Mayengo, Modeling salmonellosis transmission dynamics in humans and dairy cattle with optimal controls. Applied Mathematical Modelling, **138**, 115781 (2025).
[12] M. A. Khan, M. Farhan, S. Islam, & E. Bonyah, Modeling the transmission dynamics of avian influenza with saturation and psychological effect. Discrete & Continuous Dynamical Systems-Series S, **12**, (3), (2019).
[13] O. I. Bada, A. S. Oke, W. N. Mutuku, & P. O. Aye, Analysis of the dynamics of SI-SI-SEIR Avian influenza A (H7N9) epidemic model with re-infection. Earthline Journal of Mathematical Sciences, **5**(1), 43-73, (2021).
[14] P. Van den Driessche, & J. Watmough, Reproduction numbers and sub-threshold endemic equilibria for compartmental models of disease transmission. Mathematical biosciences, **180**, 29-48 (2002).
[15] A. Malek, & A. Hoque, A Mathematical Model of Avian Influenza for Poultry Farm and its Stability Analysis. Applications and Applied Mathematics: An International Journal (AAM), **15**, 1-23 (2020).
[16] C. Castillo-Chavez, S. Blower, P. van den Driessche, D. Kirschner, & A. A. Yakubu, (Eds.). Mathematical approaches for emerging and reemerging infectious diseases: models, methods, and theory (Vol. 126). Springer Science & Business Media, (2002).
[17] J. P. La Salle, The stability of dynamical systems. Society for Industrial and Applied Mathematics, (1976).
[18] J. Shi, X. Zeng, P. Cui, C. Yan, & H. Chen, Alarming situation of emerging H5 and H7 avian influenza and effective control strategies. Emerging microbes & infections, **12**, 2155072 (2023).
[19] C. E. Akpan, & M. O. Ibrahim, Sensitivity Analysis for Avian Influenza (Bird Flu) Epidemic Model with Exposed class. Asian Journal of Mathematics and Applications, **15**, 1-24 (2020).
[20] M. A. Khan, S. Ullah, Y. Khan, & M. Farhan, Modeling and scientific computing for the transmission dynamics of avian influenza with half-saturated incidence. International Journal of Modeling, Simulation, and Scientific Computing, **11**, 2050035 (2020).
[21] X. Zhang, L. Zou, J. Chen, Y. Fang, J. Huang, J. Zhang, & S. Ruan, Avian influenza A H7N9 virus has been established in China. Journal of biological systems, **25**, 605-623 (2017).
[22] A. B. Gumel, Global dynamics of a two-strain avian influenza model. International journal of computer mathematics, **86**, 85-108 (2009).
[23] L. Bourouiba, A. Teslya, & J. Wu, Highly pathogenic avian influenza outbreak mitigated by seasonal low pathogenic strains: Insights from dynamic modeling. Journal of Theoretical Biology, **271**, 181-201 (2011).
[24] A.Feukouo Fossi, J. Lubuma, C. Tadmon, & B. Tsanou, Mathematical modeling and nonstandard finite difference scheme analysis for the environmental and spillover transmissions of Avian Influenza A model. Dynamical Systems, **36**, 212-255 (2021).
[25] Y. Huang, K. Xu, D. F. Ren, J. Ai, H. Ji, A. H. Ge, & H. Wang, Probable longer incubation period for human infection with avian influenza A (H7N9) virus in Jiangsu Province, China, 2013. Epidemiology & Infection, **142**, 2647-2653 (2014).
[26] M. M. Mayengo, M. Kgosimore, & S. Chakraverty, Fuzzy dynamical system in alcohol-related health risk behaviors and beliefs. Soft Computing in Interdisciplinary Sciences, 109-127, (2022).
[27] C. Kirkeby, & M. P. Ward, A review of estimated transmission parameters for the spread of avian influenza viruses. Transboundary and Emerging Diseases, **69**, 3238-3246 (2022).
[28] J. C. Lagarias, J. A. Reeds, M. H. Wright, & P. E. Wright, Convergence properties of the Nelder–Mead simplex method in low dimensions. SIAM Journal on optimization, **9**, 112-147 (1998).
[29] P. H. Hobbelen, A. R. Elbers, M. Werkman, G. Koch, F. C. Velkers, A. Stegeman, & T. J. Hagenaars, Estimating the introduction time of highly pathogenic avian influenza into poultry flocks. Scientific Reports, **10**, 12388 (2020).
[30] P. J. Bonney, S. Malladi, A. Ssematimba, E. Spackman, M. K. Torchetti, M. Culhane, , & C. J. Cardona, Estimating epidemiological parameters using diagnostic testing data from low pathogenicity avian influenza infected turkey houses. Scientific reports, **11**, 1602 (2021).
[31] B.Sara, Z. Omar, T. Abdessamad, R. Mostafa, & F. Hanane, Parameters' estimation, sensitivity analysis and model uncertainty for an influenza a mathematical model: case of Morocco. Commun. Math. Biol. Neurosci., 2020, Article-ID, (2020).
[32] A. Simancas-Racines, S. Cadena-Ullauri, P. Guevara-Ramírez, A. K. Zambrano, & D. Simancas-Racines, Avian influenza: strategies to manage an outbreak. Pathogens, **12**, 610 (2023).
[33] H.Trazias, J. I. Irunde, M. Kgosimore, & M. M. Mayengo, Dynamics of Salmonellosis and the impacts of contaminated dairy products and environments: Mathematical modeling perspective and parameter estimation. Ecological Modelling, **497**, 110862 (2024).

[34] F. A. Mgandu, S. Mirau, N. Nyerere, E. Mbega, & F. Chirove, Mathematical model to assess the impacts of aflatoxin contamination in crops, livestock and humans. Scientific African, **23**, e01980 (2024).
[35] C. Ruoja, M. Mayengo, N. Nyerere, & F. Nyabadza, Modeling the influence of fear and patients' attitudes on the transmission dynamics of tuberculosis. Modeling Earth Systems and Environment, **11**, 1-16 (2025).
[36] J. Ward, J. W. Lambert, T. W. Russell, J. M. Azam, A. J. Kucharski, S. Funk, & W. J. Edmunds, Estimates of epidemiological parameters for H5N1 influenza in humans: a rapid review. medRxiv, 2024-12, (2024).
[37] A. Ssematimba, S. Malladi, P. J. Bonney, St. K. M. Charles, H. C. Hutchinson, M. Schoenbaum, & C. J. Cardona, Estimating the time of Highly Pathogenic Avian Influenza virus introduction into United States poultry flocks during the 2022/24 epizootic. PloS one, **19**, e0310733 (2024).

Serapia P. Soka earned her M.Sc. in Applied Mathematics from the Catholic University of Eastern Africa (CUEA), Kenya, in 2020. Her research interests focus on mathematical modeling of Shiga Toxin Incorporating the Environment. She is currently pursuing her doctorate in Applied Mathematics and Computational Sciences at The Nelson Mandela African Institution of Science and Technology, Arusha, Tanzania.

Maranya Mayengo completed his Master's and PhD degrees in Applied Mathematics Computational Science and Engineering at the Nelson Mandela African Institution of Science and Technology (NM-AIST)in 2014 and 2021 respectively. His research interests focus on mathematical modeling of health related issues. He currently holds the position of Senior Lecturer in the School of Computational and Communication Science and Engineering at The Nelson Mandela African Institution of Science and Technology, Arusha, Tanzania.

Moatlhodi Kgosimore completed his Ph.D. in Mathematics from the University of Botswana in 2004, focusing on the role of vaccination and treatment interventions in the spread of HIV/AIDS. Prior to this, he completed an M.Sc. in Mathematics (Mathematical Modelling) at the University of Zimbabwe in 1998 and a B.Sc. in Mathematics at the University of Botswana in 1995. His research interests focus on the mathematical modeling of infectious diseases affecting both humans and animals. He has been actively involved with the Southern Africa Mathematical Sciences Association (SAMSA).